Appl. Phys. A 75, 315–323 (2002)
DOI: 10.1007/s003390201340

Applied Physics A
Materials Science & Processing

H. WANG[1]
G. OSTER[2,✉]

Ratchets, power strokes, and molecular motors

[1] University of California, Department of Applied Mathematics and Statistics, Santa Cruz, CA 95064, USA
[2] University of California, Departments of Molecular & Cellular Biology, and ESPM, Berkeley, CA 94720-3112, USA

Received: 24 October 2001/Accepted: 11 February 2002
Published online: 22 April 2002 •

ABSTRACT We present a method for determining the effective driving potential for a molecular motor from measurements of its stochastic position versus time. In developing the method we can make precise the previously vague notions of 'Brownian ratchet' and 'power stroke', and suggest means to experimentally distinguish between the two. In particular, we distinguish between two kinds of ratchets: ratchets that rectify large fluctuations and ratchets that bias small fluctuations.

PACS 87.10.+e

1 Introduction

In 1969, Huxley proposed a theory for how the crossbridges in muscle generate the force that drives muscle contraction [1]. His model was built around the idea of capturing Brownian fluctuations in an elastic element to generate a unidirectional force; it was the first application of the 'Brownian ratchet' idea to a protein motor.[1] The idea resurfaced in the early 1990s by several groups who presented models for extracting mechanical work from isothermal Brownian motion [3, 5–8]. Some of these models were based on the notion of a 'flashing potential' that alternated stochastically between two different driving potentials [5, 8–10]. The transition between the potentials is driven by a chemical reaction. These models are part of a widely accepted mathematical formalism within which the energy transduction of molecular motors is generally studied [11]. Within this framework, it is possible to make a precise distinction between ratchet and power strokes, and even to devise methods that, in principle, could be used to distinguish experimentally between them. This is what we endeavor to do here.

In Sect. 2 we set up a mathematical framework within which the terms 'ratchet' and 'power stroke' can be defined precisely. Then in Sect. 3 we present a method by which a phenomenological 'driving potential' can be defined from experimentally measured time series of motor position versus time. For concreteness, we will use rotary motors as examples, in particular, the F_1 ATPase [12]; the extension to linear motors is obvious. We also discuss the phenomenological distinction between power stroke and ratchet, which is largely a matter of the amount of free-energy change in each ratchet step. For example, the binding of an ATP molecule to a catalytic site proceeds by a progressive annealing of hydrogen bonds that captures thermal fluctuations of the catalytic site to induce conformational changes [12–14]. This process is driven by biasing thermal fluctuations, and so could be said to be a ratchet. However, because the free-energy change in each small step (the annealing of a hydrogen bond) is not much larger than $k_B T$, the rotation of the F_1 motor driven by the ATP binding looks like a power stroke.

2 Ratchets and power strokes

Roughly speaking, a ratchet is a motor in which the motion is driven directly by thermal fluctuations and rectified, or biased, by chemical reactions. In contrast, a power-stroke motor directly drives the motion.[2] To make the definitions precise, we consider all torques (or forces for linear motors) to act on the load that the motor is driving. In this paper, the 'load' means the object the motor is driving, not the external torque acting on the motor. For example, in the rotation experiments of the F_1 ATPase, the load is the long actin filament attached to the γ subunit (see Fig. 1a and [15]). Similarly, in kinesin experiments the motor tows a large bead (the load) [16]. Typically, there are three stochastic torques acting on the load, as shown in Fig. 1b: the Brownian torque, the viscous drag torque, and the motor torque. There may also be an external conservative torque acting on the load; in experiments, this would be calibrated so as to be non-stochastic and nearly independent of motor position, such as a laser-trap-implemented force clamp [17]. The theoretical distinction between these

✉ E-mail: goster@nature.berkeley.edu

[1] The term 'Brownian ratchet' is frequently attributed to Feynman; however, the phrase – or the related term 'thermal ratchet' – never appears in his oft-cited chapter on the 'ratchet and pawl' (Chapt. 46 of the *Feynman Lectures*) [2]. To the best of our knowledge, the term 'Brownian ratchet' was first used by Simon et al. [3] to describe the isothermal trapping of Brownian fluctuations to drive protein translocation. Vale and Oosawa [4] proposed a thermal trapping scheme for molecular motors; however, it was based on thermal gradients within proteins, rather than isothermal Brownian motion.

[2] Mathematically, if thermal fluctuations are eliminated from a model while the drag coefficient is kept constant, a power stroke will still work but a ratchet will not. Of course, this makes no sense physically since the drag coefficient depends on thermal motions.

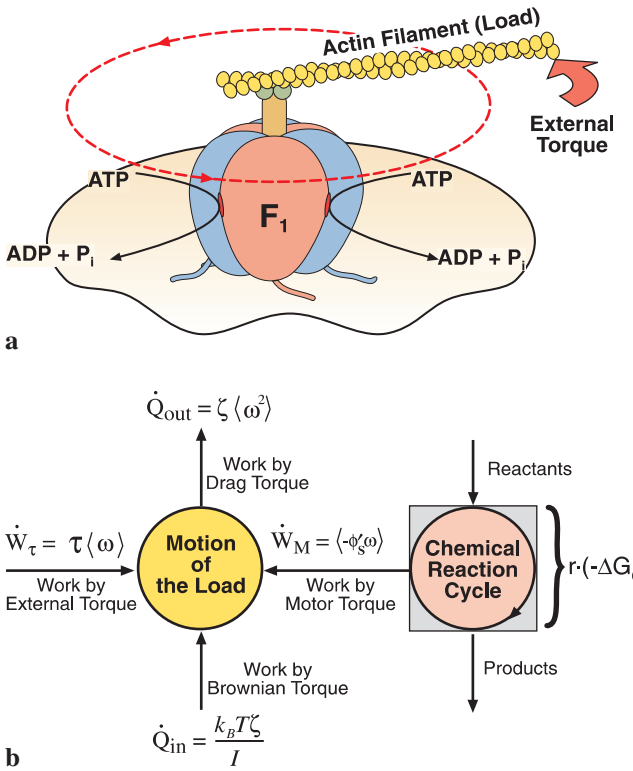

FIGURE 1 **a** Schematic of the F_1 ATPase motor experiments of Noji et al. [18]. A long actin filament (the load) is attached to the rotating shaft. There are three catalytic sites in the motor that alternate in sequence to hydrolyze ATP to ADP and phosphate, supplying the energy to turn the shaft. The motor rotates 360° in three steps, each step consuming one ATP. In principle (although not yet in the experiments), the load can be forced by an external conservative torque, such as a laser trap. **b** Four torques acting on the load of a protein motor: the Brownian torque, viscous drag torque, motor torque and the external torque. At equilibrium, in the absence of chemical reactions and external forcing, $\dot{Q}_{\rm in} = \dot{Q}_{\rm out}$, or $k_{\rm B}T = I\langle\omega^2\rangle$ (equipartition)

torques is clear. The external torque is the torque on the load from the external agent (for example, a laser trap). The motor torque is the torque on the load from the motor (in the F_1 motor experiments, the torque on the actin filament from the γ subunit). Both the drag torque and the Brownian torque derive from the surrounding fluid. As in the Langevin formulation, we use the product of the drag coefficient and the instantaneous velocity as the drag torque. The remaining torque from the surrounding fluid is the Brownian force. In practice, it may be very difficult to distinguish these torques experimentally.

The energy to drive the motion ultimately comes from chemical reactions taking place in the catalytic site(s) of the motor. However, the motor torque generated by these chemical reactions may not be directly responsible for moving the load forward. If the motor torque from the chemical reaction blocks the backward fluctuations of the load, the load will move forward driven solely by its own Brownian motion. We shall use the work done on the load per unit time by the motor torque to measure its direct contribution to the motion, and use it to distinguish between a power stroke and a ratchet.

To facilitate a quantitative discussion, we introduce a general mathematical formulation describing molecular motors [19–21]. Generally, a chemically driven molecular motor contains one or more sites wherein a chemical-reaction cycle takes place. These reactions are mechanically coupled to the rest of the protein in a fashion that depends on the particular molecular structure. In the case of the F_1 motor, there are three catalytic sites that hydrolyze ATP sequentially. Our previous modeling studies showed that ATP binding drives a hinge-bending motion in the β subunits [12]. The stochastic motion of the motor can be described by a Langevin equation. For a rotary motor (for example, F_1), the mechanical state of the system can be specified by a single angular position and momentum pair:

$$\frac{{\rm d}\theta}{{\rm d}t} = \omega, \quad \frac{{\rm d}p}{{\rm d}t} = \underbrace{-\zeta\omega}_{\substack{\text{Viscous}\\ \text{drag torque}}} \quad \underbrace{-\phi'_{\mathbf{S}}(\theta)}_{\substack{\text{Motor torque in}\\ \text{chemical state } \mathbf{S}}} \quad \underbrace{+\tau}_{\substack{\text{External}\\ \text{torque}}} \quad \underbrace{+\tau_{\rm B}(t)}_{\substack{\text{Brownian}\\ \text{Torque}}}. \tag{1}$$

Here I is the moment of inertia, ω the instantaneous angular velocity, $p = I\cdot\omega$ the angular momentum, ζ the drag coefficient, τ the external torque, and $\tau_{\rm B}(t)$ the stochastic Brownian torque.

In (1), $\phi_{\mathbf{S}}(\theta)$ is the driving potential corresponding to the current chemical state $\mathbf{S}$, $\phi'_{\mathbf{S}} \equiv \partial\phi_{\mathbf{S}}/\partial\theta$. In one reaction cycle there are N chemical states. For example, the hydrolysis cycle at each catalytic site in F_1 can be described by four chemical states $\mathbf{S}$={Empty, ATP bound, ADP+phosphate, ADP}. In the j-th chemical state, the motor is driven by $\phi_j(\theta)$, a periodic potential with period $= \Lambda$. In most cases, Λ is an integral multiple of the motor step, which we denote by Θ. The chemical reaction drives the motor by switching among this set of N potentials. Since chemical reactions are much faster than any mechanical motion of the motor, the chemical reactions can be described by a discrete Markov model, symbolically written as [21]:

$$\frac{{\rm d}\mathbf{S}}{{\rm d}t} = \mathbf{K}(\theta)\cdot\mathbf{S}. \tag{2}$$

The elements of the transition matrix $\mathbf{K}(\theta)$ are the kinetic transition rates, k_{ij}, which may depend on the motor's spatial position, θ. Conservation of probability requires that the transition matrix $\mathbf{K}(\theta)$ satisfy $\sum_{j=1}^{N} k_{ij} = 0$.

When only the average quantities of the motor behavior are sought, it is more convenient to consider the evolution of the probability density. Let $\varrho_j(\theta, p, t)$ be the probability density for finding the motor at position θ with angular momentum p in the j-th chemical state at time t. $\varrho_j(\theta, p, t)$ is governed by a set of coupled Fokker–Planck equations ensuring the conservation of probability [20–22]:

$$\frac{\partial\varrho_j}{\partial t} = -\frac{\partial}{\partial\theta}\left[\frac{p}{I}\varrho_j\right] + \frac{\partial}{\partial p}\left[\left(\phi'_j - \tau + \zeta\frac{p}{I}\right)\varrho_j\right] + \zeta k_{\rm B}T\frac{\partial^2\varrho_j}{\partial p^2} + \sum_{i=1}^{N} k_{ij}\varrho_i, \quad j = 1, 2, \ldots, N. \tag{3}$$

The average of a quantity $X_{\mathbf{S}}(\theta, p, t)$ is determined by computing

$$\langle X_{\mathbf{S}}(\theta, p, t)\rangle \equiv \int_0^{\Lambda}\int_{-\infty}^{\infty}\sum_{j=1}^{N} X_j(\theta, p, t)\varrho_j(\theta, p, t)\,{\rm d}p\,{\rm d}\theta. \tag{4}$$

As in (1), the subscript '**S**' represents the current chemical state, indicating that X may vary with the chemical state of the motor. Using (4) on (3) we can derive the energy balance on the load at the steady state. First, the steady state of (3) is found by setting the left side to zero. Then multiplying (3) by $p^2/(2I)$ and summing over the chemical states, $j = 1, \ldots, N$, we have

$$\begin{aligned} 0 = &-\frac{I}{2}\frac{\partial}{\partial\theta}\left[\left(\frac{p}{I}\right)^3\sum_{j=1}^{N}\varrho_j\right] \\ &+\frac{I}{2}\left(\frac{p}{I}\right)^2\frac{\partial}{\partial p}\left[\sum_{j=1}^{N}\left(\phi_j' - \tau + \zeta\frac{p}{I}\right)\varrho_j\right] \\ &+\zeta k_{\mathrm{B}}T\frac{I}{2}\left(\frac{p}{I}\right)^2\frac{\partial^2}{\partial p^2}\left[\sum_{j=1}^{N}\varrho_j\right]. \end{aligned} \tag{5}$$

Next, integrate (5) with respect to θ and p; because everything is periodic, the integral of the first term is zero. Applying integration by parts to the second and third terms yields:

$$\begin{aligned} 0 = &-\int_0^{\Lambda}\int_{-\infty}^{\infty}\sum_{j=1}^{N}(\phi_j' - \tau + \zeta\omega)\omega\varrho_j\,\mathrm{d}p\,\mathrm{d}\theta \\ &+\frac{\zeta k_{\mathrm{B}}T}{I}\int_0^{\Lambda}\int_{-\infty}^{\infty}\sum_{j=1}^{N}\varrho_j\,\mathrm{d}p\,\mathrm{d}\theta \\ = &\underbrace{\langle -\phi_{\mathbf{S}}'\omega\rangle}_{\dot{W}_{\mathrm{M}}} + \underbrace{\tau\langle\omega\rangle}_{\dot{W}_E} - \underbrace{\zeta\langle\omega^2\rangle}_{\dot{Q}_{\mathrm{out}}} + \underbrace{\frac{\zeta k_{\mathrm{B}}T}{I}}_{\dot{Q}_{\mathrm{in}}}. \end{aligned} \tag{6}$$

A similar approach was used to study the heat conduction via fluctuations of a mechanical device linking two temperature reservoirs [23].

Each term in (6) has the physical interpretation shown in Fig. 1b.

- $\dot{W}_{\mathrm{M}} = \langle -\phi_{\mathbf{S}}'\omega\rangle$ is the rate of work done on the load by the motor torque ($\tau_{\mathrm{M}} = -\phi_{\mathbf{S}}'$). This is the rate at which energy flows from the chemical reaction site to the load. We will see later that this rate can be positive or negative. Surprisingly, it can also exceed the rate of free-energy consumption of the motor! Note that the motor torque is stochastic since it varies with the position and the chemical state of the motor.
- $\dot{W}_E = \tau\langle\omega\rangle$ is the rate of work done on the load by the external torque.
- $-\dot{Q}_{\mathrm{out}} = -\zeta\langle\omega^2\rangle$ is the rate of work done on the load by the drag torque. Because the drag torque always opposes the motion, $-\dot{Q}_{\mathrm{out}}$ is always negative, i.e. $\dot{Q}_{\mathrm{out}} \geq 0$. $\dot{Q}_{\mathrm{out}}$ is the rate at which the kinetic energy of the load is converted by viscous friction to heat in the surrounding fluid.
- $\dot{Q}_{\mathrm{in}} = \zeta\frac{k_{\mathrm{B}}T}{I}$ is the rate of work done on the load by the Brownian torque. This is the rate at which heat is absorbed from the surrounding fluid by the load via thermal fluctuations. Part of the heat absorbed by the load becomes kinetic energy of the load, which is quickly converted by viscous friction to heat in the surrounding fluid. For molecular motors, $\dot{Q}_{\mathrm{in}}$ is much larger than the free-energy consumption rate (see below).
- The rate of free-energy consumption of the motor is $r(-\Delta G_{\mathrm{C}})$ where r is the rate of chemical reaction in the motor and ΔG_{C} is the free-energy change in one reaction cycle. At physiological conditions, ΔG_{C} of ATP hydrolysis cycle is about –20 $k_{\mathrm{B}}T$ [24]. For a 1-μm actin filament rotating around one end, $\dot{Q}_{\mathrm{in}} = \zeta\frac{k_BT}{I} \approx 3.85\times10^{10}\,k_BT/\mathrm{s}$. In contrast, the maximum ATPase activity of the F_1 motor is about 300 ATPs per second [15]. That gives an upper bound on the energy consumption rate of the F_1 motor: $r(-\Delta G_{\mathrm{C}}) \leq 6\times10^3\,k_BT/\mathrm{s}$. Thus, for the F_1 motor, $\dot{Q}_{\mathrm{in}}$ is much larger than $r\cdot(-\Delta G_{\mathrm{C}})$. This is generally true for all molecular motors.

The net rate of heat flow from the load to the surrounding fluid at temperature T is

$$\dot{Q}_{\mathrm{out}} - \dot{Q}_{\mathrm{in}} = \zeta\langle\omega^2\rangle - \frac{\zeta k_{\mathrm{B}}T}{I} = \frac{\zeta k}{I}\left(\frac{I\langle\omega^2\rangle}{k} - T\right).$$

In [25], $\dot{Q}_{\mathrm{out}} - \dot{Q}_{\mathrm{in}}$ was called 'the dissipation of energy to the heat bath'. However, as illustrated by the example in Fig. 2 below, $\dot{Q}_{\mathrm{out}} - \dot{Q}_{\mathrm{in}}$ may exceed the energy consumption. Because ω is the instantaneous angular velocity of the load, we can define the temperature of the load as $T_{\mathrm{L}} = I\langle\omega^2\rangle/k_{\mathrm{B}}$. Thus

$$\dot{Q}_{\mathrm{out}} - \dot{Q}_{\mathrm{in}} = \frac{\zeta k_{\mathrm{B}}}{I}(T_{\mathrm{L}} - T). \tag{7}$$

Using (6), we can express $\dot{W}_{\mathrm{M}}$ in terms of $\dot{Q}_{\mathrm{out}} - \dot{Q}_{\mathrm{in}}$:

$$\dot{W}_{\mathrm{M}} = \dot{Q}_{\mathrm{out}} - \dot{Q}_{\mathrm{in}} - \tau\langle\omega\rangle. \tag{8}$$

(8) describes the energy flow through the load. When $\tau = 0$ and $\dot{W}_{\mathrm{M}} > 0$, energy flows from the chemical reaction site to the load via the motor torque, and then to the surrounding fluid where it ends up as heat. This case corresponds to a power-stroke motor working against only the viscous drag. When $\dot{W}_{\mathrm{M}} = 0$ and $\tau < 0$ (i.e. the external torque opposes the motion), heat flows from the surrounding fluid to the load via thermal fluctuations, and then to the external agent that exerts the torque τ on the load. This case corresponds to a ratchet motor working against an external conservative torque (a spring or a laser trap). Thermal energy is extracted from the surrounding fluid and is used to increase the potential energy of the external agent. This energetically unfavorable process is rectified by the chemical reactions in the motor. Notice that the chemical reactions do not directly drive the load: the work done on the load by the motor torque is zero.

With the above definitions, one can view a motor as having a power-stroke component and a ratchet component by calculating the fraction of the total free-energy consumption used for each component:

$$\begin{aligned} f_{\mathrm{P}} &\equiv \frac{\dot{W}_{\mathrm{M}}}{r\cdot(-\Delta G_{\mathrm{C}})} = \text{percent power stroke}, \\ f_{\mathrm{R}} &\equiv 1 - \frac{\dot{W}_{\mathrm{M}}}{r\cdot(-\Delta G_{\mathrm{C}})} = \text{percent ratchet}, \end{aligned} \tag{9}$$

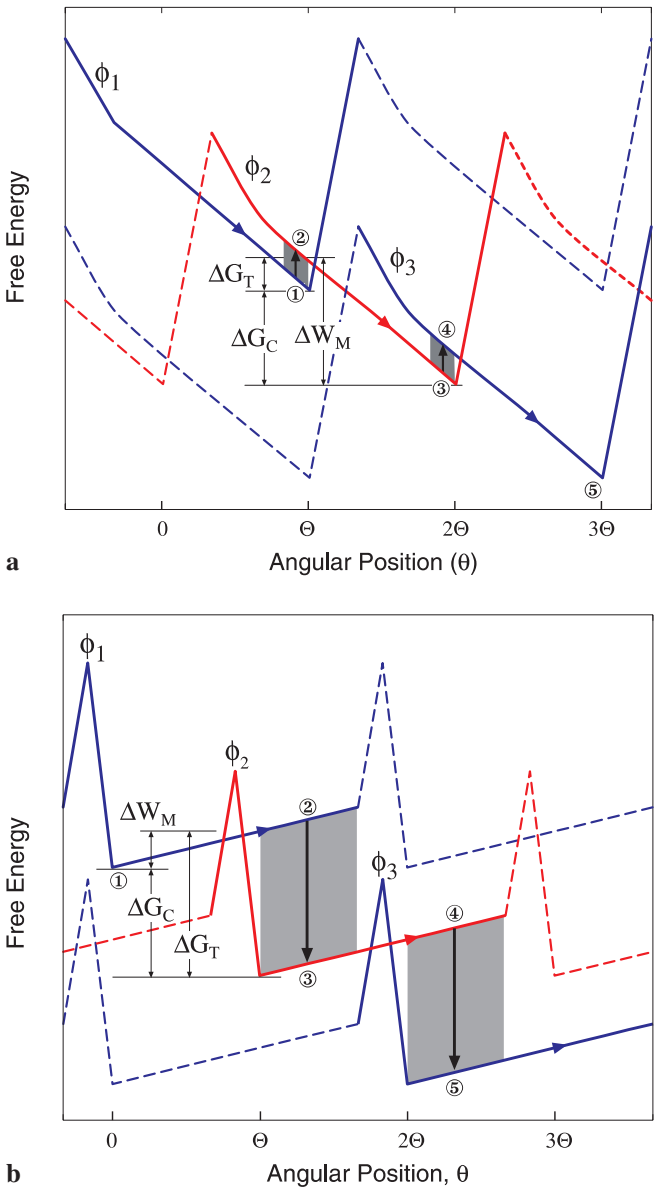

FIGURE 2 Two example motor systems. The arrows along the potentials and in the shaded regions indicate the positive direction of the motor. ΔG_C is the free-energy change in one reaction cycle (①→②→③). ΔW_M is the work done on the load by the motor torque in one reaction cycle. ΔG_T is the free-energy change in the transition between potentials in the positive direction of the motor. **a** A motor system with $-\Delta G_C = 16 k_B T$, $\Delta G_T = 4 k_B T$ and $\Delta W_M = 20 k_B T$. According to the definition (9) this motor has a 125% power-stroke component and a (−25%) ratchet component: $f_P = 125\%$ and $f_R = -25\%$. This is an over-simplified model for the F_1 motor at low ATP concentrations (see the discussion accompanying Fig. 3). **b** A motor system with $-\Delta G_C = 16 k_B T$, $\Delta G_T = -20\, k_B T$ and $\Delta W_M = -4\, k_B T$. This motor has a (−25%) power-stroke component and a 125% ratchet component: $f_P = -25\%$ and $f_R = 125\%$. This may be viewed as a simplified model for a polymerization ratchet motor

Thus the motor can be viewed formally as the sum of two motors: one driven by power strokes consuming a portion f_P of the total energy consumption, and the other driven by a Brownian ratchet using f_R of the total energy consumption: $f_P + f_R = 1$. Note that, as defined, f_P or f_R individually can be positive or negative, and can even be larger than 1. The interpretation is as follows:

- If $0 \le f_P \le 1$ and $0 \le f_R \le 1$, both the power-stroke component and the ratchet component are driving the motor motion.
- If $f_P < 0$, the power-stroke component is working against the motor motion.
- If $f_R < 0$, the ratchet component is working against the motor motion.

If one insists on labeling a protein motor as either a power-stroke motor or a ratchet motor, one must choose an arbitrary threshold (say, $f_0 = 50\%$): if $f_P < f_0$, we call the motor a ratchet motor, otherwise we call it a power-stroke motor.

2.1 *Examples of energy flows through a molecular motor*

Figure 2 shows two hypothetical motor systems driven by moving along a series of identical periodic potentials, each shifted to the right by Θ in the θ direction, and by ΔG_C down in free energy. All protein motors coordinate the reaction steps with the mechanical cycle; therefore, we restrict the transition between potentials to take place only in the shaded regions. Only three successive potentials are shown for each motor system in Fig. 2. However, it is clear that as the motor goes forward the free energy of the system decreases.

Note that potentials in the collection $[\phi_1, \phi_3, \phi_5, \dots]$ differ only by a shift downwards in free energy, so they have the same effect on the motor motion. If we use ϕ_1 to represent $[\phi_1, \phi_3, \phi_5, \dots]$ and ϕ_2 to represent $[\phi_2, \phi_4, \phi_6, \dots]$, we can treat these two motor systems mathematically as systems switching between two potentials. This is the usual representation; however, we will not adopt this convention since it obscures the monotonic decrease in free energy.

In Fig. 2a, because the free-energy change in the transition ① → ② is positive, the motion ② → ③ down the potential does more work on the load than the free energy consumed in one reaction cycle: $\Delta W_M > (-\Delta G_C)$. Consequently, the power-stroke component of the motor is larger than 100%: $f_P = \Delta W_M/(-\Delta G_C) > 100\%$. The percentage of the ratchet component is negative. This situation arises because the transition ① → ② is energetically unfavorable – it presents a barrier to the motor motion. Thus, the motor system shown in Fig. 2a can be viewed as a strong power-stroke component working against a weak ratchet component. This is the situation in the V-ATPase proton pumps, and in the bacterial ATP synthase under anaerobic conditions when the F_1 motor drives the F_o motor backwards [12, 26].

In Fig. 2b, forward motion of the motor requires it to diffuse up the potential ϕ_1: ① → ②. During this motion, thermal energy is absorbed by the load from the surrounding fluid, so the work done on the load by the motor torque is negative: $\Delta W_M < 0$. Consequently, the percentage of the power stroke is negative, and the percentage of the ratchet component is larger than 100%. The transition from ϕ_1 to ϕ_2 (② → ③) is energetically favorable, and the potential ϕ_2 rectifies the diffusive motion ① → ② up the potential ϕ_1. So in this motor, each individual potential is trying to drive the motor backwards, but the chemical transition between potentials rectifies large forward fluctuations and thus effectively drives the motor forward. The motor system shown in Fig. 2b can be viewed as a strong ratchet component working against a weak power-

stroke component. This is the normal situation in ATP synthase wherein the F_o motor drives the F_1 motor 'backwards' to synthesize ATP.

2.2 *What is measurable?*

While the above classification of 'power stroke' and 'ratchet' is well defined, there are problems associated with using $\dot{W}_M$ to measure the power-stroke component of a motor. First, $\dot{W}_M$ is not directly measurable in experiments. In the absence of an external torque ($\tau = 0$), $\dot{W}_M$ is equal to the net rate of heat flow from the load to the surrounding fluid (c.f. (7) and (8)):

$$\dot{W}_M = \dot{Q}_{out} - \dot{Q}_{in} = \frac{\zeta k_B}{I}(T_L - T). \tag{10}$$

In theory, both T_L and T can be measured, and $\dot{W}_M$ can be evaluated. However, this approach is not practical for molecular motors because $\zeta k_B/I$ is very large, and consequently the temperature difference $T_L - T$ is very small. For example, in the F_1 rotation experiments, an actin filament is attached to the rotating γ shaft of F_1 motor to visualize the rotation [15]. For a 1-μm actin filament rotating around one end, $\zeta k_B/I = 1.58 \times 10^{11}\,\mathrm{pN\,nm\,s^{-1}\,K^{-1}}$. Although $\dot{W}_M$ may exceed $r(-\Delta G_C)$, generally $\dot{W}_M$ is of the same order as $r(-\Delta G_C)$. At physiological conditions, $-\Delta G_C$ of ATP hydrolysis cycle is $80 \sim 90$ pN nm/s [24]. When the F_1 motor is driving a 1-μm actin filament at saturated ATP concentrations, the hydrolysis activity is about 20 ATP/s [15]. That corresponds to a free-energy consumption rate of < 2000 pN nm/s. Even if $\dot{W}_M$ is 10 times the free-energy consumption rate (which is very unlikely), the temperature difference between the load and the surrounding fluid is still very small:

$$T_L - T = \frac{\dot{W}_M}{(\zeta k_B/I)} < 3.8 \times 10^{-5}\,\mathrm{K}. \tag{11}$$

To estimate $\dot{W}_M$ from the temperature difference $T_L - T$ requires measuring the temperature difference with an accuracy of at least 10^{-5} K.

The second problem with using $\dot{W}_M$ is that it is a quantity averaged over long time (or over a large ensemble). If a motor has a 100% or more power-stroke component, it implies that the amount of work done on the load in one reaction cycle by the motor torque exceeds the free-energy consumption. However, it does not tell us whether the work is done uniformly over one motor step or only in a certain fraction of a motor step. If the work is done nearly uniformly over one motor step, as in the example shown in Fig. 2a, then the load is directly driven by the motor torque over the entire motor step. If the work is done only during a small fraction of a motor step, then the load is directly driven by the motor torque only during that fraction of the motor step. For the rest of the motor step, the load depends on thermal fluctuations to carry it forward. Therefore, a motor with 100% or more power-stroke component does not necessarily mean that the motor torque directly drives the load forward over the entire duration of each motor step.

To remedy these two defects, we consider an alternative definition of power stroke and ratchet based on the effective driving potential of the motor, which is a measurable quantity.

3 The effective driving potential

We first consider a simplified version of (3). Because molecular motors operate in the high-friction limit, we may ignore the inertial term if the instantaneous velocity of the motor is not sought. When the inertia term is omitted, the Langevin (1) reduces to

$$\zeta \frac{d\theta}{dt} = -\phi_S'(\theta) + \tau + \tau_B(t). \tag{12}$$

(2) stays the same. The corresponding Fokker–Planck equation is

$$\frac{\partial \varrho_j}{\partial t} = D\frac{\partial}{\partial \theta}\left[\frac{\phi_j' - \tau}{k_B T}\varrho_j + \frac{\partial \varrho_j}{\partial \theta}\right] + \sum_{i=1}^{N} k_{ij}\varrho_i, \;\; j = 1, 2, \ldots, N. \tag{13}$$

Consider the steady-state solution of (13). Summing over all the chemical states, j, and letting $\varrho = \sum_{j=1}^{N} \varrho_j$, we obtain:

$$0 = D\frac{\partial}{\partial \theta}\left[\frac{\psi' - \tau}{k_B T}\varrho + \frac{\partial \varrho}{\partial \theta}\right], \quad \psi' = \sum_{j=1}^{N} \phi_j' \frac{\varrho_j}{\varrho}. \tag{14}$$

(14) shows that the probability density ϱ behaves as if the motor is driven by a potential, ψ. For this reason, we define ψ as the effective driving potential (EDP) of the motor.

Because both ϕ_j' and ϱ_j are periodic, ψ' is periodic and ψ can be written as

$$\psi(\theta) = \phi(\theta) - \frac{\Delta\psi(\Theta)}{\Theta}\theta, \quad \Delta\psi(\Theta) = \psi(0) - \psi(\Theta). \tag{15}$$

Here $\phi(\theta)$ is a periodic function with period equal to the motor step, Θ. $\Delta\psi(\Theta)$ can be viewed as the effective driving energy per motor step. In Appendix A we show that the effective driving energy per motor step is bounded by the free-energy consumption per motor step:

$$\Delta\psi(\Theta) \le \frac{\Theta}{\langle\omega\rangle} r(-\Delta G_C). \tag{16}$$

Inequality (16) is not a trivial statement: consider the fact shown above that the work done by the motor torque can exceed the free-energy consumption!

3.1 *An example of how to use the EDP*

Because ϕ_j and ϱ_j are not readily observable in experiments, the definition does not provide us a practical way to estimate the EDP. However, if enough data are collected, ϱ can be estimated. Then the EDP ψ can be constructed from ϱ using (14). In Appendix B, we give a prescription for constructing ψ from a time series of motor positions. Here we illustrate the method described in Appendix B. Because there is no published data sequence of motor positions available for real motors, we use the hypothetical motor system shown in Fig. 2a as an example. To generate a sequence of motor positions, we run a Langevin simulation of (12) and (2) with the potentials shown in Fig. 2a. In the simulation, we use $\Theta = 2\pi/3$, $\tau = 0$, and $D = 4\,\mathrm{rad^2/s}$, which corres-

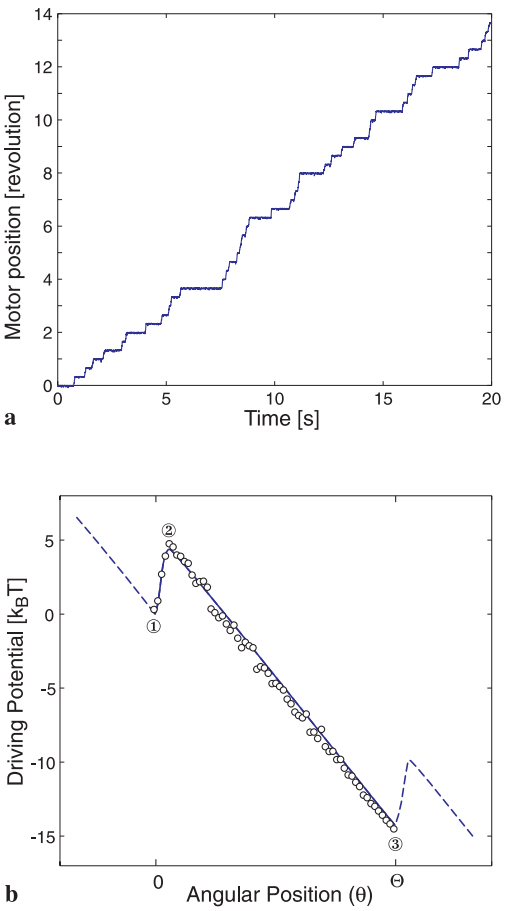

FIGURE 3 **a** A sequence of 5000 motor positions over a time period of 20 s generated in a Langevin simulation of the system shown in Fig. 2a. **b** The exact EDP (*lines*) and the reconstructed EDP (*hollow circles*). The simulated sequence of motor positions shown in (**a**) is used as 'data' to reconstruct the EDP. The exact EDP is obtained by solving the Fokker–Planck equation (13)

ponds to the diffusion constant of a 1-μm actin filament rotating around one end (see Fig. 1a). A sequence of 5000 motor positions in a time period of 20 s is shown in Fig. 3a. We use this sequence as 'data' and apply the method described in Appendix B to reconstruct the EDP. Both the exact EDP computed from (14) and the reconstructed EDP are shown in Fig. 3b. The reconstructed EDP agrees with the exact one very well.

The hypothetical system in Fig. 2a can be viewed as an over-simplified model for the F_1 motor at low ATP concentration [12]. The motion ② → ③ down the potential represents the ATP binding transition that drives the rotation of the γ shaft. The transition ① → ② represents several chemical reaction steps including hydrolysis, product release and the diffusion of the next ATP into the catalytic site. The free-energy change associated with the transition ① → ② is affected by the ATP concentration in solution. When the ATP concentration is low, the diffusion of an ATP into the catalytic site is entropically unfavorable, and the dwell time of the motor near ① increases because it takes longer to capture the next ATP from solution. Thus the motor sees a free-energy barrier near ①. This is reflected in the EDP shown in Fig. 1b, which has an energy barrier followed by a downhill slope.

3.2 *Distinguishing between power stroke and ratchet, based on the effective driving potential*

The distinction between power stroke and ratchet based on the EDP is not exactly the same as the distinction based on the work done on the load by the motor torque discussed in Sect. 2. The EDP is an average of N driving potentials corresponding to N chemical states. In the process of averaging, information about the work done on the load by the motor torque is lost. Similarly, information about the precise role of thermal excitations is also lost. This can be illustrated by looking at the EDP in Fig. 3b. The potential shows an energy barrier followed by a downhill slope. The downhill slope can be viewed as a power stroke by the motor torque. However, the uphill energy barrier could be attributed to two possible factors:

1. It may be a barrier on the driving potential associated with one chemical state. To surmount it, the load has to capture large thermal fluctuations. In the process of the load fluctuating up the barrier, the work done on the load by the motor torque is negative.
2. It may be an energy barrier in one step of the chemical reaction. It could be either an enthalpic activation barrier in the catalytic step, or an entropic barrier caused by the low concentrations of reactants diffusing into catalytic sites. An enthalpic activation barrier is overcome by the thermal energy captured at the catalytic sites. An entropic barrier is overcome by the random diffusion of the reactants to the catalytic site. In either case, in the process of overcoming a barrier in the chemical reaction, the work done on the load by the motor torque is zero. This is the case for the hypothetical motor system shown in Fig. 2a.

Therefore, by looking at the EDP alone, it is not possible to tell where the thermal energy is absorbed and in what way it is used to overcome the barrier. Nevertheless, from the EDP we can deduce which part of the motor step is driven by the motor torque and which part depends on thermal excitations. For the EDP shown in Fig. 3b, ① → ② depends on thermal excitations, and ② → ③ is driven by a power stroke.

For an EDP ψ, we consider a constant-torque power stroke that has the same effective driving energy per step as ψ : $\tau_\psi = \Delta\psi(\Theta)/\Theta$. This constant-torque power stroke is the most efficient way to utilize the energy to drive the load [27]. At each position, θ, we compare $\psi'(\theta)$ with τ_ψ, and define the relative contributions of the power stroke and thermal excitations as follows:

$$C_{\mathrm{PS}}(\theta) \equiv \max\left(\min\left(\frac{-\psi'(\theta)}{\tau_\psi}, 1\right), 0\right),$$

$$C_{\mathrm{PS}} \equiv \frac{1}{\Theta}\int_0^\Theta C_{\mathrm{PS}}(\theta)\,\mathrm{d}\theta,$$

$$C_{\mathrm{TE}} \equiv 1 - C_{\mathrm{PS}}.$$

Figure 4 shows various driving potentials and the corresponding values of C_{PS} and C_{TE}. The potential ψ_{D} consists of a series of small steps; each small step has a free-energy change of the order of $k_{\mathrm{B}}T$. If we align potentials ψ_{C} and ψ_{D}, they are close to one another on a free-energy scale much larger than $k_{\mathrm{B}}T$, although ψ_{C} is a power stroke and ψ_{D} is a ratchet. It may

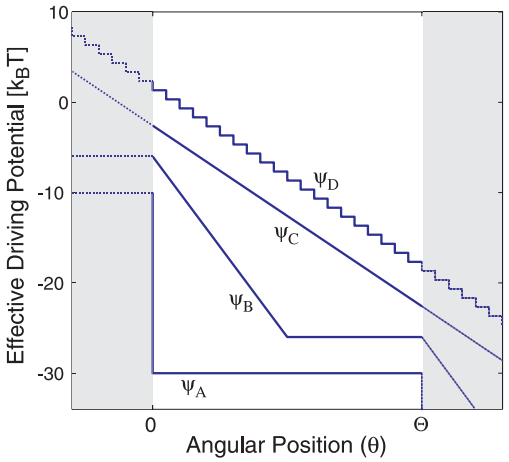

FIGURE 4 Various driving potentials and corresponding values of C_{PS} and C_{TE}. For ψ_A, $C_{PS} = 0$ and $C_{TE} = 100\%$: the entire motor step is driven by thermal excitations. For ψ_B, $C_{PS} = 50\%$ and $C_{TE} = 50\%$: half of the motor step is driven by a power stroke, the other half is driven by thermal excitations. For ψ_C, $C_{PS} = 100\%$ and $C_{TE} = 0$: the entire motor step is driven by a power stroke. For ψ_D, $C_{PS} = 0\%$ and $C_{TE} = 100\%$: the entire motor step is driven by thermal excitations. However, ψ_D has the same phenomenological behavior as ψ_A (see the text for more discussion of ψ_A and ψ_D)

be possible – but not easy – to distinguish between ψ_C and ψ_D. There are two difficulties. First, the difference between ψ_C and ψ_D is small. To distinguish between ψ_C and ψ_D, we need to reconstruct ψ_C and ψ_D with high accuracy, which requires a very large collection of accurately measured data. Second, even if ψ_D is the motor driving potential, the EDP accurately reconstructed from the load positions may be virtually the same as ψ_C because the protein elasticity between the motor and the load can easily smooth out small unevenness on the potential [28]. Therefore, it is probably fruitless to try and distinguish ψ_C from ψ_D. Instead, we can consider distinguishing between potentials ψ_A and ψ_D. Both are ratchets, but they are very different. ψ_A has a large free-energy change associated with each step, whereas ψ_D has a small step size and a small free-energy change associated with each step. Thus ψ_A drives the load by rectifying infrequent large fluctuations whereas ψ_D drives the load by slightly biasing frequent small fluctuations. When driven by ψ_A, once the load fluctuates beyond one step, the probability of going backwards is extremely small because of the large free-energy drop associated with each step in ψ_A. When driven by ψ_D, the load can fluctuate forward and backwards. Because the free-energy change associated with each step is of the order of k_BT, the probability of going backwards is only slightly smaller than that of going forward. Thus, ψ_D does not prevent the load from going backwards at all. On the other hand, because of the small step size, the frequency of fluctuating one step forward is high. That is why we say ψ_D drives the load by slightly biasing frequent small fluctuations. Therefore, it is more meaningful to distinguish between ratchets that rectify infrequent large fluctuations and ratchets that slightly bias frequent small fluctuations. The latter have the same phenomenological behavior as power strokes.

4 Conclusions

Roughly speaking, a ratchet is a motor that is driven directly by thermal fluctuations. The chemical reaction in a ratchet motor does not contribute directly to the motor motion. Instead, it rectifies or biases the forward fluctuations. However, a precise definition of ratchets depends on how one measures the contribution of thermal fluctuations. In this paper, two definitions are considered. The first definition (discussed in Sect. 2) is based on the amount of work done per motor step by the motor torque. Because the work done by the stochastic motor torque is not directly measurable in experiments, this definition is meaningful only if we know the details of the motor mechanism. The second definition (discussed in Sect. 3) is based on the fraction of a motor step that depends on thermal excitations. We formulated a procedure for reconstructing an effective driving potential for a molecular motor from experimental data. Because the effective driving potential involves averaging over all chemical states, the information about the work done on the load by the motor torque is lost. However, the effective driving potential can be used to determine what portion of the motor step is driven by thermal excitations. This leads to a phenomenological distinction between a Brownian ratchet and a power stroke. This phenomenological distinction depends on the free-energy scale being considered and the possible experimental measurements. In particular, ratchets that slightly bias frequent small fluctuations are phenomenologically indistinguishable from power strokes. On the other hand, ratchets that rectify infrequent large fluctuations are very different from power strokes. In light of our analysis, we suggest that it is useful to distinguish between these two very different kinds of ratchets.

ACKNOWLEDGEMENTS This work was supported by NSF grants DMS-0077971 (HW) and DMS-9972826 (GO).

Appendices

Appendix A Proof of inequality (16)

Here we present the mathematical proof leading to inequality (16). First we rewrite (13) in a slightly different form:

$$\frac{\partial \varrho_j}{\partial t} = -\frac{\partial J_j}{\partial \theta} + I_{j-1/2} - I_{j+1/2}, \quad j = 1, 2, \ldots, N \tag{A.1}$$

$$J_j = -D\left[\frac{\phi_j' \varrho_j}{k_B T} - \frac{\tau \varrho_j}{k_B T} + \frac{\partial \varrho_j}{\partial \theta}\right] = -D\varrho_j\left(F_j' - \frac{\tau}{k_B T}\right),$$

$$F_j = \frac{\phi_j}{k_B T} + \ln(\varrho_j)$$

$$I_{j+1/2} = \varrho_j k_{j\to j+1} - \varrho_{j+1} k_{j+1\to j}. \tag{A.2}$$

Here, J_j is the probability flux density in the θ direction for the j-th state, and $I_{j+1/2}$ is the probability flux density in the chemical reaction direction from state j to state $j+1$. The transition rates $k_{j\to j+1}$ and $k_{j+1\to j}$ satisfy detailed balance at equilibrium:

$$\frac{k_{j\to j+1}(\theta)}{k_{j+1\to j}(\theta)} = \exp\left(\frac{\phi_j(\theta) - \phi_{j+1}(\theta)}{k_B T}\right). \tag{A.3}$$

Since the motor operates in a chemical and mechanical cycle, the boundary conditions for (A.1) are periodic in both

coordinates:

$$\phi_j(\theta+\Theta,t)=\phi_j(\theta,t),\quad \varrho_j(\theta+\Theta,t)=\varrho_j(\theta,t)$$
$$\phi_{N+j}=\phi_j+\Delta G_{\mathrm{C}},\quad \varrho_{N+j}=\varrho_j. \tag{A.4}$$

We consider the steady state of (A.1). The average velocity is given by $\langle\omega\rangle=\Theta\left(\sum_{j=1}^{N}J_j\right)$. The effective driving energy per motor step is

$$\Delta\psi(\Theta)=-\int_0^{\Theta}\frac{1}{\varrho}\sum_{j=1}^{N}\phi_j'\varrho_j\,\mathrm{d}\theta=\frac{k_{\mathrm{B}}T}{D}\int_0^{\Theta}\frac{1}{\varrho}\sum_{j=1}^{N}J_j\,\mathrm{d}\theta-\tau\Theta. \tag{A.5}$$

At the steady state $\sum_{j=1}^{N}J_j$ is independent of θ: therefore, $\langle\omega\rangle\Delta\psi(\Theta)$ can be expressed as

$$\langle\omega\rangle\Delta\psi(\Theta)=\frac{\Theta k_{\mathrm{B}}T}{D}\int_0^{\Theta}\frac{1}{\varrho}\left(\sum_{j=1}^{N}J_j\right)^2\mathrm{d}\theta-\langle\omega\rangle\tau\Theta. \tag{A.6}$$

Applying the Cauchy–Schwarz inequality to $\sum_{j=1}^{N}J_j=\sum_{j=1}^{N}\left[\varrho_j^{1/2}\cdot\varrho_j^{1/2}D\left(F_j'-\tau/k_{\mathrm{B}}T\right)\right]$, we obtain

$$\begin{aligned}\frac{1}{\varrho}\left(\sum_{j=1}^{N}J_j\right)^2&\le\sum_{j=1}^{N}\varrho_jD^2\left(F_j'-\frac{\tau}{k_{\mathrm{B}}T}\right)^2\\&\equiv-D\sum_{j=1}^{N}J_j\left(F_j'-\frac{\tau}{k_{\mathrm{B}}T}\right).\end{aligned} \tag{A.7}$$

Integrating by parts and using (A.1), then summing by parts and using (A.4), we have

$$\begin{aligned}\int_0^{\Theta}\frac{1}{\varrho}\left(\sum_{j=1}^{N}J_j\right)^2\mathrm{d}\theta&\le D\int_0^{\Theta}\sum_{j=1}^{N}F_jJ_j'\,\mathrm{d}\theta+D\int_0^{\Theta}\sum_{j=1}^{N}J_j\frac{\tau}{k_{\mathrm{B}}T}\,\mathrm{d}\theta\\&=D\int_0^{\Theta}\sum_{j=1}^{N}F_j(I_{j-1/2}-I_{j+1/2})\,\mathrm{d}\theta+\frac{D\langle\omega\rangle\tau}{k_{\mathrm{B}}T}\\&=D\int_0^{\Theta}\sum_{j=1}^{N}I_{j-1/2}(F_j-F_{j-1})\,\mathrm{d}\theta+\frac{D(-\Delta G_{\mathrm{C}})}{k_{\mathrm{B}}T}\int_0^{\Theta}I_{1/2}\,\mathrm{d}\theta+\frac{D\langle\omega\rangle\tau}{k_{\mathrm{B}}T}.\end{aligned} \tag{A.8}$$

The first integral on the right side of (A.8) is negative:

$$I_{j-1/2}(F_j-F_{j-1})=\varrho_{j-1}k_{j-1\to j}(1-G)\ln(G)\le0,$$
$$G=\frac{\varrho_j}{\varrho_{j-1}}\exp\left(\frac{\phi_j-\phi_{j-1}}{k_{\mathrm{B}}T}\right).$$

The second integral is the chemical reaction rate r. Thus, (A.8) becomes

$$\int_0^{\Theta}\frac{1}{\varrho}\left(\sum_{j=1}^{N}J_j\right)^2\mathrm{d}\theta\le\frac{D(-\Delta G_{\mathrm{C}})}{k_{\mathrm{B}}T}r+\frac{D\langle\omega\rangle\tau}{k_{\mathrm{B}}T}. \tag{A.9}$$

Combining (A.6) and (A.9) yields

$$\langle\omega\rangle\Delta\psi(\Theta)\le\Theta r(-\Delta G_{\mathrm{C}}), \tag{A.10}$$

which leads to inequality (16).

Appendix B Constructing the effective driving potential (EDP)

Here we discuss the method for constructing the EDP from a time series of motor positions.

Suppose in experiments we record a sequence of times and motor positions $\{(t_i,\theta_i),i=1,2,\ldots,M\}$. These could be the motor positions at equally spaced times or at random times. First, the average angular velocity of the motor is estimated as

$$\langle\omega\rangle\approx\frac{\theta_{\mathrm{M}}-\theta_1}{t_{\mathrm{M}}-t_1}. \tag{B.1}$$

Then we shift each θ_i by an integral multiple of Θ into the internal $[0,\Theta]$, where Θ is the motor step size. The resulting sequence $\{\theta_i,i=1,2,\ldots,M\}$ represents the probability density distribution of the motor position. Let us divide $[0,\Theta]$ into n bins of equal size $\Delta\theta=\Theta/n$. Let m_k be the number of motor positions in the sequence that fall in the k-th bin $[(k-1)\Delta\theta,k\Delta\theta]$. Let p_k be the probability that the motor position is in the k-th bin. m_k/M is a good approximation for p_k if the sequence contains enough samples.

$$p_k\approx\frac{m_k}{M}. \tag{B.2}$$

To reconstruct ψ, we discretize the Fokker–Planck (14) as a Markov chain [20, 21]:

$$\frac{\langle\omega\rangle}{\Theta}=p_kF_k-p_{k+1}B_k,\quad k=1,2,\ldots,n. \tag{B.3}$$

The forward (F_k) and backwards (B_k) transition rates are given by

$$F_k=\frac{D}{(\Delta\theta)^2}\frac{\alpha_k}{\exp(\alpha_k)-1},\quad B_k=\frac{D}{(\Delta\theta)^2}\frac{-\alpha_k}{\exp(-\alpha_k)-1}, \tag{B.4}$$

where

$$\alpha_k=\frac{(\Delta\psi)_k-\tau\Delta\theta}{k_{\mathrm{B}}T},$$
$$(\Delta\psi)_k=\psi\left(\left(k+\frac{1}{2}\right)\Delta\theta\right)-\psi\left(\left(k-\frac{1}{2}\right)\Delta\theta\right). \tag{B.5}$$

This discretization is second-order accurate when ψ is smooth. More importantly, it preserves detailed balance: this

ensures that the scheme behaves well even if ψ has sharp jumps.

Once we know $\langle\omega\rangle$ and p_k, we can numerically solve for $(\Delta\psi)_k$ using (B.3), (B.4) and (B.5) for $k = 1, 2, \ldots, n$. From this the EDP ψ is constructed:

$$\psi\left(\left(k+\frac{1}{2}\right)\Delta\theta\right) = \sum_{j=1}^{k}(\Delta\psi)_j, \quad k = 1, 2, \ldots, n. \qquad \text{(B.6)}$$

Because the potential is only determined up to a constant, here we have set $\psi(\Delta\theta/2) = 0$.

REFERENCES

1 A. Huxley, R. Simmons: Nature **233**, 533 (1971)
2 R. Feynman, R. Leighton, M. Sands: *The Feynman Lectures on Physics* (Addison-Wesley, Reading, MA 1963)
3 S. Simon, C. Peskin, G. Oster: Proc. Nat. Acad. Sci. USA **89**, 3770 (1992)
4 R.D. Vale, F. Oosawa: Adv. Biophys. **26**, 97 (1990)
5 A. Ajdari, J. Prost: C. R. Acad. Sci. Paris **315**, 1635 (1992)
6 C.S. Peskin, G.M. Odell, G. Oster: Biophys. J. **65**, 316 (1993)
7 M.O. Magnasco: Phys. Rev. Lett. **71**, 1477 (1993)
8 C.S. Peskin, G.B. Ermentrout, G.F. Oster: Mechanochemical Coupling in ATPase Motors. In: *Interplay of Genetic and Physical Processes in the Development of Biological Form* (Springer, Les Houches 1994)
9 J. Prost, J. Chauwin, L. Peliti, A. Ajdari: Phys. Rev. Lett. **72**, 2652 (1994)
10 C. Doering, W. Horsthemke, J. Riordan: Phys. Rev. Lett. **72**, 2984 (1994)
11 A. Parmeggiani, F. Julicher, A. Ajdari, J. Prost: Phys. Rev. E **60**, 2127 (1999)
12 G. Oster, H. Wang: BBA **1458**, 482 (2000)
13 D. Koshland: Angew. Chem. **33**, 2375 (1994)
14 G. Oster, H. Wang: J. Bioenerg. Biomembr. **332**, 459 (2000)
15 R. Yasuda, H. Noji, K. Kinosita, M. Yoshida: Cell **93**, 1117 (1998)
16 M. Schnitzer, K. Visscher, S. Block: Nature Cell Biol. **2**, 718 (2000)
17 K. Visscher, M. Schnitzer, S. Block: Nature **400**, 184 (1999)
18 H. Noji, R. Yasuda, M. Yoshida, K. Kinosita: Nature **386**, 299 (1997)
19 C. Bustamante, D. Keller, G. Oster: Acc. Chem. Res. **34**, 412 (2001)
20 A. Mogilner, T. Elston, H.-Y. Wang, G. Oster: In: *Joel Keizer's Computational Cell Biology*, ed. by C.P. Fall, E. Marland, J. Tyson, J. Wagner (Springer, New York 2001)
21 H. Wang, G. Oster: Nature **396**, 279 (1998)
22 H. Risken: *The Fokker–Planck Equation.* 2nd edn. (Springer, New York 1989)
23 J. Parrondo, P. Español: Am. J. Phys. **64**, 1125 (1996)
24 B. Alberts, D. Bray, J. Lewis, M. Raff, K. Roberts, J. Watson: *Molecular Biology of the Cell,* 3rd edn. (Garland, New York 1994)
25 K. Sekimoto: J. Phys. Soc. Jpn. **66**, 1234 (1997)
26 M. Grabe, H. Wang, G. Oster: Biophys. J. **78**, 2798 (2000)
27 H.-Y. Wang, G. Oster: Europhys. Lett. **57**, 134 (2002)
28 T. Elston, C. Peskin: SIAM J. Appl. Math. **60**, 842 (2000)